Fermi National Accelerator Laboratory

FERMILAB-Conf-93/387-E

DØ

Inclusive Jet and Direct Photon Production at the DØ Experiment

Jonathan Kotcher
For the DØ Collaboration

Fermi National Accelerator Laboratory
P.O. Box 500, Batavia, Illinois 60510

Superconducting Super Collider Laboratory
2550 Beckleymeade Avenue, Dallas, Texas 75237

December 1993

Presented at the *9th Workshop on Proton-Antiproton Collider Physics*,
Tsukuba, Japan, October 18-22. 1993

Disclaimer

Inclusive Jet and Direct Photon Production at the DØ Experiment

Jonathan Kotcher
for the DØ collaboration
Superconducting Super Collider Laboratory
2550 Beckleymeade Avenue
Dallas, TX, USA 75237

Preliminary measurements of the inclusive jet and single photon production cross sections in $\bar{p}p$ collisions at $\sqrt{s} = 1.8$ TeV by the DØ experiment at the Fermilab Tevatron are reported. The inclusive jet cross sections in various pseudorapidity ranges covering $|\eta| < 3$ are presented, along with comparisons to next-to-leading order QCD predictions. The single photon cross section in the central region ($|\eta| < 0.9$) is also presented, as is a description of the conversion method used to determine the background contamination. The single photon cross section is compared to a recent next-to-leading logarithm QCD calculation.

1. Introduction

Next-to-leading order (NLO) QCD calculations include descriptions of initial and final state radiation at the parton level that are not included at leading order. The inclusion of these and other higher-order terms allows for more stringent tests of the theory. The inclusive jet cross section offers a means of testing NLO QCD over a wide range of jet energies and many orders of magnitude in the cross section, provided the experimental jet algorithm is appropriately matched to NLO parton level jet definitions.

We present below preliminary measurements of the inclusive jet cross section in $\bar{p}p$ collisions at $\sqrt{s} = 1.8$ TeV in the region $|\eta| < 0.9$ (where the pseudorapidity $\eta \equiv -\ln[\tan(\theta/2)]$, and θ is the polar angle with respect to the proton-beam direction). Comparisons with recent calculations in NLO [1], using both HMRSB0 [2] and CTEQ2M [3] parton distribution functions, are also shown. We have in addition expanded the inclusive jet measurement to $2 < |\eta| < 3$ and present these results, along with a theoretical comparison. Very preliminary results for our intercryostat region [4] ($1 < |\eta| < 2$) are also presented.

An additional probe of QCD is possible through measurement of the single photon production cross section. We present our method for determining the fraction of photons in the data after cuts, α, and show our preliminary measurement of the single photon cross section for $|\eta| < 0.9$ and photon transverse momenta $p_T^\gamma > 10.7$ GeV. The data are compared with a recent next-to-leading logarithm (NLL) QCD calculation [5].

The results contained here are based on the preliminary analysis of ≈ 15 pb^{-1} of data recorded during the 1992/93 run at the Tevatron collider, the first run for DØ. The reader is referred to Refs. [4,6] for descriptions of the detector and trigger, along with details on the jet-finding algorithm, jet energy scale corrections, and electron/photon identification techniques used at DØ.

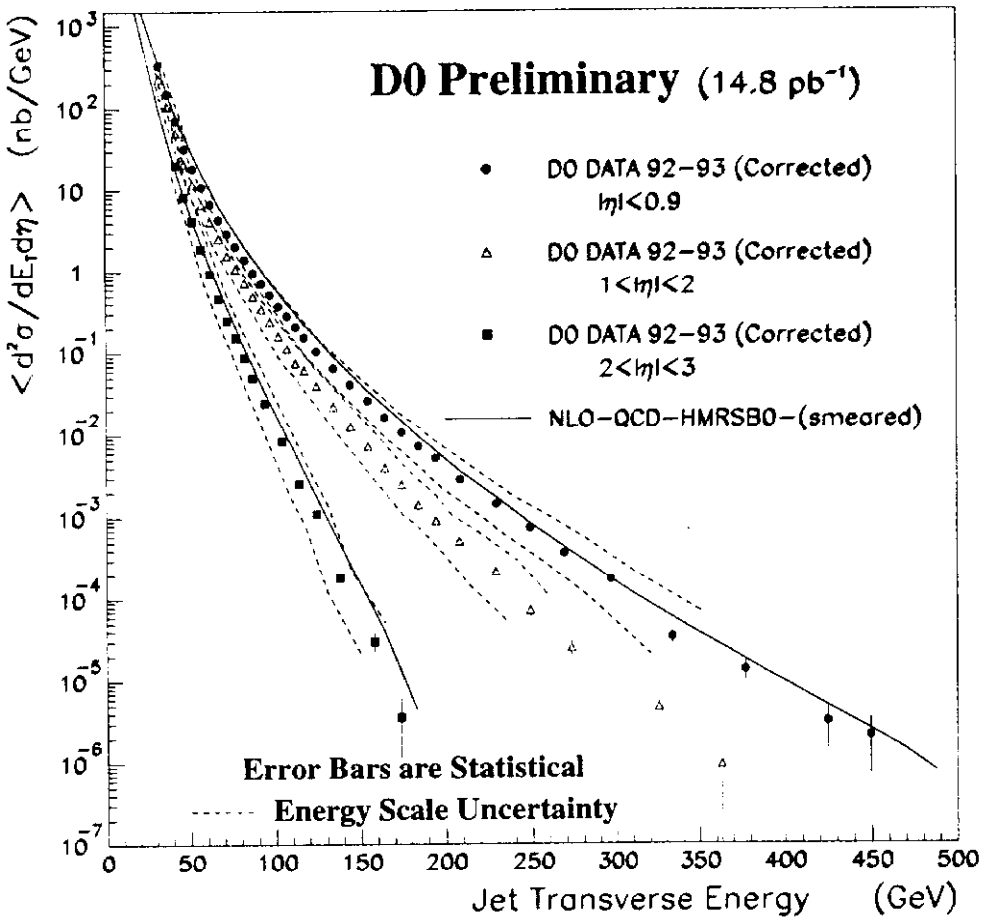

Figure 1: Preliminary inclusive jet cross section as a function of the jet transverse energy for 3 different η regions. HMRSB0 [2] parton distributions have been used in the theoretical calculation. An overall $\pm 12\%$ error in the luminosity is not included.

corrected for the z-vertex cut and the trigger prescale, and $\Delta\eta$ is the range in pseudorapidity subtended for the relevant η region.

The cross section for each of the three η regions is shown in Fig. 1. Next-to-leading order QCD calculations [1] using HMRSB0 [2] parton distributions are also shown for the central and forward regions, with the theory having been smeared by our jet energy resolution. The renormalization scale used is $\mu = p_T/2$. The dotted line indicates the jet energy scale uncertainty, which is the dominant systematic error in the measurement. The measured cross sections in both the central and forward regions agree qualitatively with the theory. Studies of the energy scale correction and cut efficiencies for jets reconstructed in the intercryostat region ($1 < |\eta| < 2$) are still underway; we therefore do not include a theoretical prediction here.

CDF has reported [8] excellent agreement between the theory calculated with this choice of parton distributions and their data for $|\eta| < 0.9$. The agreement between the data points and the theory in Fig. 1 can therefore be taken as a measure of the agreement between the DØ and CDF inclusive jet cross sections in this pseudorapidity range.

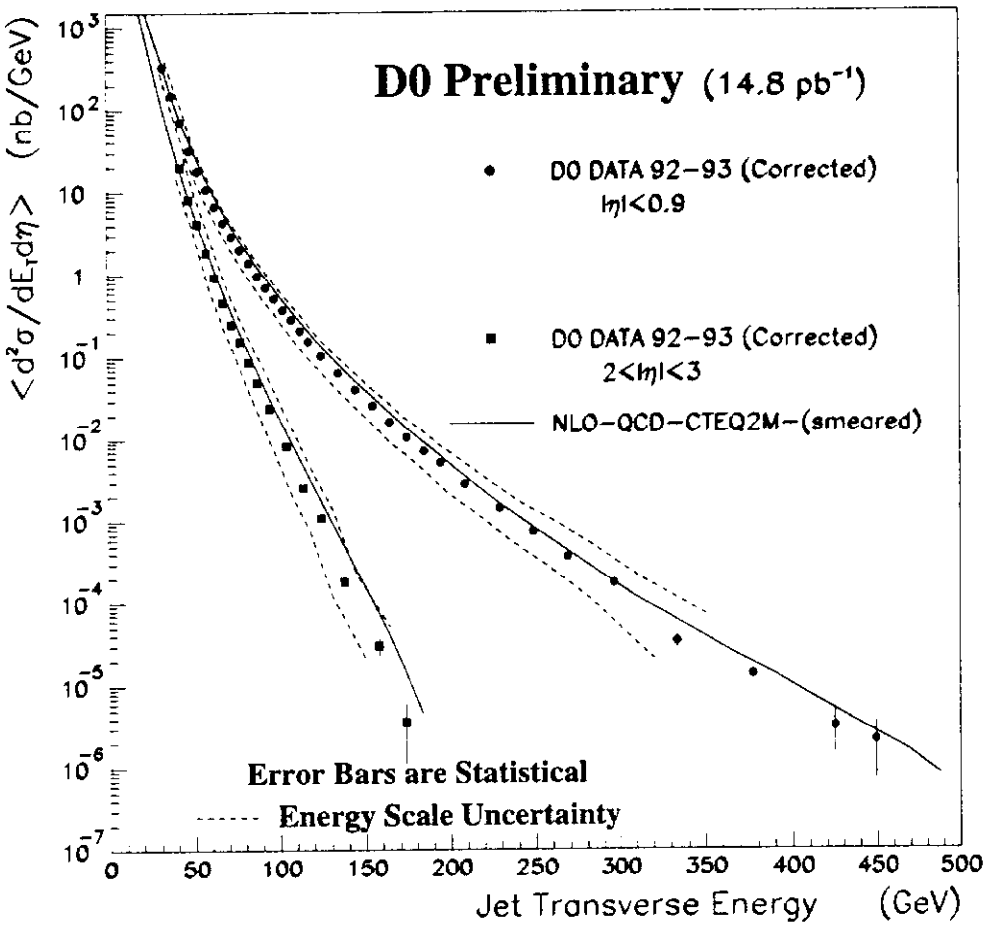

Figure 2: Same as Fig. 1, but with CTEQ2M [3] parton distributions used to calculate the theory curves.

Parton distributions have recently become available from the CTEQ collaboration [3] that use the latest experimental data to constrain the low-x behavior of the distribution functions. CTEQ2M [3] parton distributions have been used to calculate the theory curve in Fig. 2. The data in this plot is the same as that in Fig. 1; only the choice of parton distributions used to calculate the theory differs between the two. The data agree qualitatively with this theoretical prediction as well.

Our present systematic error is too large to allow us to draw quantitative conclusions about the two different parton distributions from the comparison of the data to the corresponding theory curves. Efforts to reduce this error are currently underway.

3. Direct Photons

Direct photon production is dominated at low-p_T by QCD-Compton scattering at the Born level in high energy proton-antiproton collisions. It provides a direct measure of the gluon distribution of the proton that is unencumbered by uncertainties due to the jet energy scale and fragmentation effects. The high center-of-mass energy of the Tevatron allows for

tests of QCD in a kinematic region that is characterized by low x_T ($x_T = 2p_T/\sqrt{s}$), which probes a region in Feynman-x that is populated predominantly by gluons. High-resolution, highly-segmented electromagnetic (EM) calorimetry allows for an intrinsically more precise determination of the photon energy and direction than is attainable for jets, making this a complementary, and potentially more revealing, channel in which to test the low-x behavior of the theory.

The primary experimental challenge in the measurement of the direct photon cross section is the extraction of the prompt photon signal from the copious backgrounds due to π^0 and η meson decays to photons. DØ employs a variation of the conversion method [9] to accomplish this. The method exploits the fact that multiple photons from meson decays are more likely to convert (produce e^+e^- pairs) in the material in front of the central drift chamber (CDC) than are single photons, and is described below.

3.1 Conversion Method

The conversion method as applied here is based on the following relationships:

$$N_{wtrk} = \epsilon_\gamma N_\gamma + \epsilon_\pi N_\pi + \epsilon_e N_e \tag{2}$$

$$N_{ntrk} = (1 - \epsilon_\gamma)N_\gamma + (1 - \epsilon_\pi)N_\pi + (1 - \epsilon_e)N_e \tag{3}$$

$$N = N_\gamma + N_\pi + N_e = N_{wtrk} + N_{ntrk}, \tag{4}$$

where N_{wtrk} is the number of particles in the final sample that have a track reconstructed in the CDC chamber that points to an EM calorimeter cluster, N_{ntrk} is the number of particles in the final sample with no track pointing to the EM cluster, ϵ_x is the efficiency for detecting the species of particle x with both a calorimeter cluster and a reconstructed track, N_x is the number of particles of species x in the final sample, and N is the total number of particles in the final sample. Studies of the η meson contribution to the background are currently underway, and have not yet been incorporated into the analysis. Direct photons are expected to contribute to the N_{ntrk} sample and the 2-*mip* portion of the N_{wtrk} sample (see below).

The above equations serve to define the efficiencies, and may be solved to yield an expression for the photon fraction α, defined by $N_\gamma = \alpha N$, where α is given by:

$$\alpha = \frac{\epsilon_\pi - \epsilon}{\epsilon_\pi - \epsilon_\gamma}. \tag{5}$$

The quantity ϵ is given by:

$$\epsilon = \frac{N_{wtrk}}{N} \times [1 - f(1 - \frac{\epsilon_\pi}{\epsilon_e})]. \tag{6}$$

Here, the parameter $f = \epsilon_e N_e / N_{wtrk}$. It is equal to the fraction of tracks in the N_{wtrk} sample that deposit an amount of energy in the CDC chamber consistent with that expected from a single minimum ionizing particle (i.e., 1-*mip* tracks). This fraction is obtained from a fit

to the dE/dx distribution measured in the CDC chamber. The value of f obtained from the data collected with our low-E_T trigger (see below) was (35±8)%.

We compute the efficiencies from the following relations:

$$\epsilon_e = t = \text{tracking efficiency} \tag{7}$$

$$\epsilon_\gamma = pt = (\text{probability of conversion}) \times t \tag{8}$$

$$\epsilon_\pi = \epsilon_\gamma[1 + \rho(1 - \epsilon_\gamma)]. \tag{9}$$

In this last equation, ρ is a parameter that is equal to, for a given π^0 momentum, the fraction of π^0's that decay with an opening angle less than the road size used for track reconstruction in the CDC chamber. As the momentum of the π^0 approaches 0, $\rho \to 0$, and $\epsilon_\pi \approx \epsilon_\gamma$, the efficiency for detecting a single photon. As the π^0 momentum becomes very large, $\rho \to 1$, and, for small ϵ_γ, $\epsilon_\pi \approx 2\epsilon_\gamma$, the efficiency for detecting two photons. The probability of conversion, p, is determined from a full GEANT Monte Carlo simulation of the detector. Since the material in front of the CDC varies with angle, the probability of conversion is a function of η. The average value obtained was $< p >= (12 \pm 1)\%$. The tracking efficiency was extracted from analysis of the $Z^0 \to e^+e^-$ sample. For the cuts used in this analysis, we obtained a value of $t = (62 \pm 4)\%$.

Using Eqns. (5-9), we obtained a value for α that varies from ≈ 0.36 at low p_T ($p_T^\gamma \approx 10$ GeV), to ≈ 0.98 at high p_T ($p_T^\gamma \approx 100$ GeV). The error in the cross section is dominated by the uncertainty in α, which we have estimated to be $\pm 50\%$ for $p_T^\gamma < 20$ GeV, and $\pm 30\%$ for $p_T^\gamma > 20$ GeV.

The triggers used to collect the direct photon data sample are summarized in Table 2. Offline cuts included the η cut ($|\eta| < 0.9$), a cut on missing E_T to reject W bosons ($E_T^{miss} < E_T^\gamma/2$), an isolation cut ($[E_T(\Delta R = 0.4) - E_T(\Delta R = 0.2)] < 2$ GeV), an electromagnetic shower shape cut, and a cut requiring the EM fraction in the core of the electromagnetic cluster to be $> 96\%$ of the total core energy. There were also a series of cuts against isolated noise in the calorimeter that can fake electromagnetic clusters. For the N_{wtrk} sample, additional cuts were applied requiring that there be one track reconstructed in the CDC chamber within a road about the electron direction, and that the distance between the track, extrapolated into the calorimeter, and the cluster centroid be less than 6 cm. The

Hardware Trigger 1 EM trigger tower with:	Software Trigger 1 EM cluster with:	Integrated Luminosity (nb^{-1})
$E_T > 2.5$ GeV	$E_T > 6$ GeV	5.4
$E_T > 7$ GeV	$E_T > 14$ GeV	22.3
$E_T > 14$ GeV	$E_T > 30$ GeV	3860

Table 2: Triggers used in the collection of the direct photon data sample, showing E_T thresholds and integrated luminosity included in the analysis. The software trigger includes an EM fraction cut, an isolation cut, and transverse and longitudinal shower shape cuts.

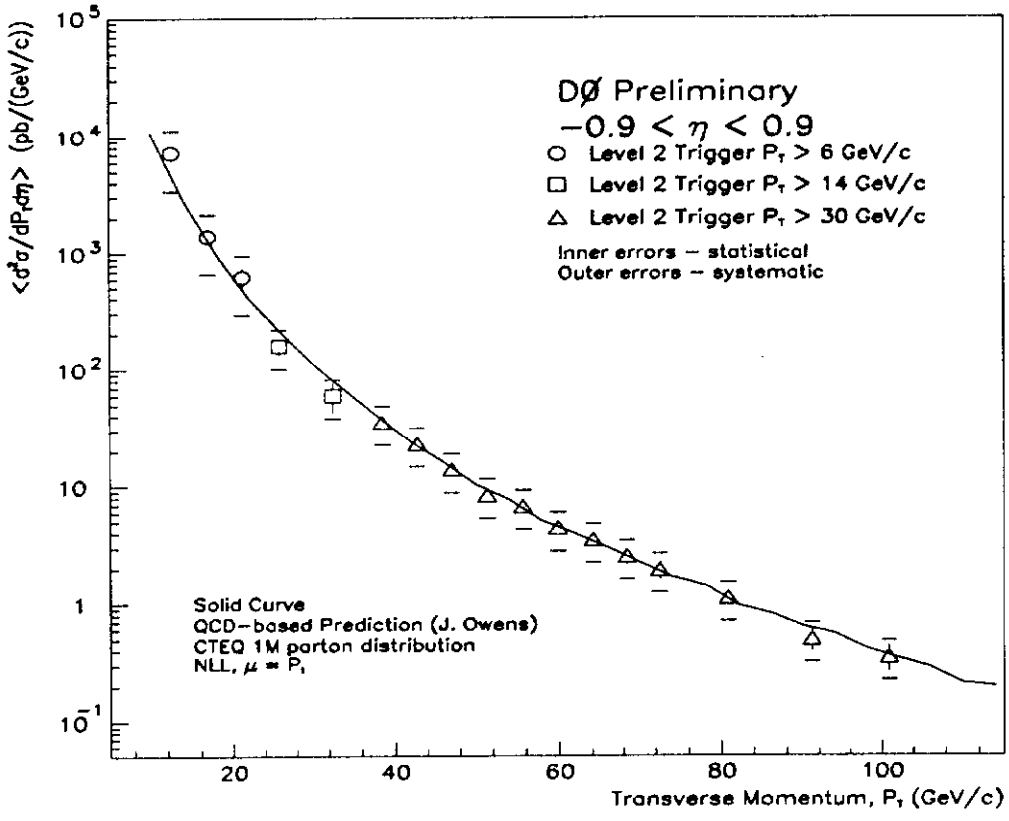

Figure 3: The single photon cross section, plotted as a function of the photon p_T, for $|\eta| < 0.9$. A next-to-leading logarithm QCD calculation [5] using CTEQ1M [3] parton distributions with $\mu = p_T$ is also shown.

offline E_T cuts for the three triggers were 10.7, 23.5, and 36.4 GeV for the low, medium, and high E_T triggers, respectively. The above cuts resulted in 5135, 270, and 3872 events having survived for these same triggers.

3.2 Single Photon Cross Section

The single photon cross section, averaged over finite p_T bins and the fiducial η region, is given by:

$$< \frac{d^2\sigma}{dp_T d\eta} >= \frac{\alpha N}{\mathcal{L}_{trig} A \epsilon_c \Delta p_T \Delta \eta}, \tag{10}$$

where α is the photon fraction, N is the number of particles in the final sample in the η interval $\Delta\eta$ with p_T in Δp_T, $\mathcal{L}_{trig}$ is the integrated luminosity for the appropriate trigger, corrected for the relevant prescale, A is the detector acceptance (computed from Monte Carlo), ϵ_c is the product of the trigger, reconstruction, and offline cut efficiencies, and $\Delta\eta$ is the η range subtended ($\Delta\eta = 1.8$). The values for A and ϵ_c used were $(91 \pm 3)\%$ and $(66 \pm 10)\%$, respectively.

Our preliminary measurement of the single photon cross section plotted as a function of

the photon p_T in the central region is shown in Fig. 3. A next-to-leading logarithm calculation [5] using CTEQ1M [3] parton distributions with $\mu = p_T$ is shown for comparison. The theory has been smeared by our measured electromagnetic energy resolution, and includes an isolation cut that has been matched to that used in the experimental analysis. The inner vertical bars on the data points reflect the statistical uncertainty, and the outer horizontal bars the systematic errors. We have included the systematic errors on α, A, and ϵ_c quoted above, along with a $\pm 12\%$ error for the luminosity, and an estimated $\pm 15\%$ error due to the uncertainty in the electromagnetic energy scale. The measured cross section agrees well with the theoretical prediction.

4. Other Studies

As alluded to above, inclusive jet measurements offer the promise of enabling us to quantitatively distinguish between different parton distributions. Studies comparing the data to theoretical predictions using a variety of different parton distributions, including those shown here, are currently underway. Measurements of the dependence of the inclusive jet cross section on the cone size used to define the jets, in conjunction with NLO QCD calculations, provide additional tests of the theory at the parton level. These studies, too, are currently being pursued.

Other ongoing studies involving photons at DØ include measurements of the diphoton cross section in the central region, searches for excited quarks and new phenomena by probing the invariant mass of the direct photon/leading jet system, further tests of QCD through measurement of the center-of-mass scattering angle between the isolated photon and the beam direction ($\cos\theta^*$ distribution), and measurement of the single photon cross section in the forward region ($1.8 < |\eta| < 3.0$). The latter measurement holds promise for constraining the low-x gluon structure functions [10].

4. References

1. S.D. Ellis, Z. Kunszt and D.E. Soper, Phys. Rev. D40 (1989) 2188.
2. A.D. Martin, R.G. Roberts and W.J. Stirling, Phys. Rev. D43 (1991) 3648-3656.
3. J. Botts *et al.*, Phys. Lett. B304 (1993) 159.
4. N. Graf, "Production of W and Z bosons at DØ", these proceedings.
5. J. Ohnemus, H. Baer and J. Owens, Phys. Rev. D42 (1990) 61.
6. H. Weerts, "Studies of Jet Production in the DØ Detector", these proceedings.
7. N.J. Hadley, "Cone Algorithm for Jet Finding", DØ internal note DØ-904 (November, 1989).
8. CDF Collaboration, FERMILAB-Conf-93/204-E (August, 1993); S. Kuhlmann, "CDF QCD Overview", these proceedings.
9. UA2 Collaboration, J.A. Appel *et al.*, Phys. Lett. B176 (1986) 239.
10. M. Demarteau, "Physics at $\bar{p}p$ Colliders", FERMILAB-Conf-92/103 (1992).